Sleep Medicine 57 (2019) 61–69

Contents lists available at ScienceDirect

Sleep Medicine

journal homepage: www.elsevier.com/locate/sleep

Original Article

Continuous positive airway pressure alters brain microstructure and perfusion patterns in patients with obstructive sleep apnea

Hillel S. Maresky [a, b, c, 1], Isaac Shpirer [b, d, 1], Miriam M. Klar [a, b, *], Max Levitt [a, b, e], Efrat Sasson [f], Sigal Tal [a, b]

[a] Department of Radiology, Assaf Harofeh Medical Center, Zerifin, Israel
[b] Sackler Faculty of Medicine, Tel Aviv University, Tel Aviv, Israel
[c] Department of Medical Imaging, Hospital for Sick Children, University of Toronto, Toronto, Ontario, Canada
[d] Sleep and Snoring Clinic, Assaf Harofeh Medical Center, Zerifin, Israel
[e] Department of Surgery, Division of Urology, Ottawa General Hospital, University of Ottawa, Ottawa, Ontario, Canada
[f] WiseImage, Hod Hasharon, Israel

ARTICLE INFO

Article history:
Received 29 May 2018
Received in revised form
29 September 2018
Accepted 20 December 2018
Available online 31 January 2019

Keywords:
Obstructive sleep apnea
Continuous positive airway pressure
MRI perfusion
Cerebral blood flow
Diffusion tensor imaging

ABSTRACT

Objectives: To assess the effects of continuous positive airway pressure (CPAP) treatment on brain structure and function in patients with obstructive sleep apnea (OSA).
Methods: A prospective study of seven OSA patients recruited from the sleep center at our institution was carried out. Patients were treated with six weeks of CPAP treatment. Pre-treatment and post-treatment magnetic resonance imaging (MRI) perfusion scans were obtained and compared to assess for treatment-induced changes. Microstructural changes were quantified using functional anistrophy (FA) and mean diffusivity (MD), and brain perfusion was quantified using cerebral blood flow (CBF) and cerebral blood volume (CBV).
Results: Of the seven patients included the in study, six (85.7%) were male, and the mean age was 51 years (standard deviation = 13.14). Increased FA and decreased MD were found in the hippocampus, temporal lobes, fusiform gyrus, and occipital lobes. Decreased FA and increased MD were found in frontal regions for all patients ($p < 0.05$). Increased CBF and CBV were also observed following treatment ($p < 0.05$).
Conclusion: In addition to symptom resolution, CPAP treatment may allow for healing of OSA-induced brain damage as seen by restoration of brain structure and perfusion.

1. Introduction

Obstructive sleep apnea (OSA) is the most common sleep disorder [1], with an estimated prevalence ranging from 4 to 32.8% [2–5]. Increasing prevalence has been observed [4], with a prediction for continued increase due to the increasing obesity prevalence in North America [6,7]. OSA presents as snoring, frequent episodes of sleep interruption, excessive daytime sleepiness, hypoxemia, hypercapnia, swings in intra-thoracic pressure and increases sympathetic activity [1,8,9].

There is limited knowledge regarding the pathogenesis of OSA [10]. Although, it is known that the OSA-induced hypoxemia-reoxygenation pattern causes vascular oxidative stress, leading to profound alterations in cerebral autoregulation [8]. This results in loss of vasodilatory mechanisms [11] and subsequent alterations in cerebral blood flow (CBF) and perfusion pressure [8], and ultimately reduced CBF [11]. This may place OSA patients at risk for cerebral ischemia and stroke [8]. Furthermore, studies have indicated white matter changes on routine magnetic resonance imaging (MRI) of these patients, possibly due to this cerebral ischemia [11], however, these white matter changes have not been consistently observed across all studies. Furthermore, patients with OSA have a significantly slower rate of recovery of blood pressure, CBF velocity, and cerebrovascular conductance than those without OSA, likely due to impaired autoregulatory mechanisms [8].

* Corresponding author. Project Manager of Neuroradiology Research, Department of Radiology, Assaf Harofeh Medical Center, Zerifin, Israel.
E-mail address: miriamklar@mail.tau.ac.il (M.M. Klar).
[1] These authors contributed equally to this work.

https://doi.org/10.1016/j.sleep.2018.12.027

If left untreated, long-term sequelae of OSA include hypertension, cardiovascular morbidities, insulin resistance, decreased cognitive function, mood, quality of life, and premature death [1,2,4,6,8,10,12]. First-line treatment for OSA consists of continuous positive airway pressure (CPAP) therapy [13], and studies have shown it has the ability to not only prevent the development of hypertension, but can also reduce blood pressure in OSA patients [14,15]. Similarly, arrhythmias caused by OSA can be attenuated with CPAP treatment [16–18]. In addition, CPAP treatment has positive effects on OSA patients suffering from heart failure [19,20]. Furthermore, CPAP has also been shown to reduce cognitive impairment seen in OSA patients [21] and acutely attenuate sympathetic drive [7].

Given CPAP's relief and reversal of OSA symptoms, investigation into the effects of CPAP through brain imaging is underway, although these methods are largely limited to transcranial Doppler, T1-weighted imaging, and functional MRI (fMRI) [22–27]. These neuroimaging techniques allow for assessment of functional changes in the brain [28–30], whereas diffusion tensor imaging (DTI) differs from other neuroimaging techniques in that it allows for the observation of brain microstructural changes [28–31]. Parameters used include (1) fractional anistrophy ((FA), the measure of microstructural integrity; increased in regions of high myelination, dense axonal packing, and white matter maturation but decreased in regions of axonal degeneration and demyelination); (2) mean diffusivity ((MD), a description of membrane density that is sensitive to cellularity, edema, and necrosis and decreased in regions of high myelination, dense axonal packing, and white matter maturation but increased in regions of axonal degeneration and demyelination), (3) CBF; and (4) cerebral blood volume (CBV). By analyzing these parameters, DTI gives information regarding brain injury and repair [29,30], thereby making DTI an important tool for assessing pathology and pathophysiology of diseases and treatments, which cannot be done through transcranial Doppler, T1-weighted imaging, and fMRI.

DTI has proven successful at describing the damage and treatment-induced changes in traumatic brain injury [30,32–34]. More recently, DTI has started being applied to better describe and understand the changes and pathogenesis of OSA [35–37]. We hypothesize that CPAP treatment will induce structural and perfusion changes in the brains of patients suffering from OSA. This study uses DTI and dynamic susceptibility contrast (DSC) imaging (a sub-type of DTI) to assess for these changes by comparing pre- and post-treatment brain images.

2. Methods

2.1. Overview

The current study is a prospective cohort study of patients suffering from OSA. The study was approved by the hospital's Institutional Review Board (IRB#: 0060-15-ASF) and informed consent forms were obtained from each patient.

All patients who were diagnosed with OSA at our institution and candidates for CPAP treatment were considered for inclusion in the study. OSA is defined as the repetitive closure of the upper airway during sleep [2,8] resulting in five or more apneic events per hour [3,6], with an apneic event defined as the cessation of airflow through the nose and mouth for >10 seconds [38]. OSA diagnoses were made using overnight polysomnography (PSG). Patients less than 18 years of age, pregnant, with a body mass greater than 300 kg (due to an MRI scanner limitation), and those suffering from cognitive impairment were excluded from the study. Following application of inclusion and exclusion criteria, 10 patients were randomly selected to participate in the study.

Patients included in the study underwent six weeks of CPAP treatment during sleeping hours. CPAP settings were determined for each patient by auto-titration with a portable system (Autotest, ResMed, Sydney, Australia) during overnight PSG. Analysis of the pressure that included 90% of the events with a leak lower than 0.4 L/s was used to determine optimal CPAP pressure. CPAP usage time was electronically downloaded to assess adherence to treatment (defined as >4 h of CPAP per night during the study period). Information regarding patient demographics, PSG statistics, and patient co-morbidities was collected from patient files and recorded.

2.2. MRI scan protocol

All patients underwent MRI before CPAP treatment and after CPAP treatment. MRI scans were performed on a 3- Tesla system (MAGNETOM Skyra, Siemens Medical Solutions, Germany) with a multichannel head coil as a receiver coil. The MRI protocol included T2 weighted, T1 weighted, fluid-attenuated inversion recovery (FLAIR), susceptibility weighted imaging (SWI) DSC, and DTI.

DTI scan sequence parameters included 30 diffusion weighted images scanned with different gradient directions (b = 1000) and one volume without diffusion weighting, with the following parameters: TR = 10,300 ms, TE = 89 ms, voxel size = 1.8 × 1.8, matrix = 128 × 128, number of slices = 63, slice thickness = 2.2 mm.

DSC scan sequence parameters included 50 T2*-weighted gradient-echo echo planar imaging (EPI) volumes, two repetitions before a bolus injection of Gadolinium-DTPA (Gd-DTPA) and 48 repetitions after injection of Gd-DTPA. Sequence parameters: TR = 2300 ms, TE = 40 ms, flip angle = 30°, voxel size = 1.8 × 1.8, matrix = 128 × 128, number of slices = 25, slice thickness = 3.9 mm.

2.3. MRI analysis

DTI analysis included motion and EPI correction and regularization of the DWI volumes as well as calculation of DTI maps (MD and FA) were performed using Explore-DTI software [39]. DSC analysis included motion correction and was performed using SPM software (version 12, UCL, London, UK). DSC analysis was performed as described in previous studies [40,41] using in-house software written in Matlab R2016b (Mathworks, Natick, MA, USA). MRI signal intensity was converted to Gd concentration, fitted to the gamma variate function and deconvolved on a voxel-by-voxel basis to calculate the CBF, CBV, and mean transit time (MTT) maps. The maps were normalized to the median image intensity in order to compensate for differences in the injection procedure. A more detailed description is found in the supplementary material.

2.4. Voxel-based analysis

Voxel-based analysis was performed comparing DSC parameters before and after CPAP treatment. Spatial normalization and statistical analysis were performed using the SPM software (version 12, UCL, London, UK). For DTI, spatial normalization was performed for each patient based on the mean DWI image with similar contrast to the template used in SPM (ICBM template, based on T1 contrast). The normalization parameters were applied on the DTI maps. Spatial smoothing with kernel size of 8 mm full width half maximum was applied. For DSC, spatial normalization was performed for each patient based on the first DSC volume (ICBM template). The normalization parameters were applied on the DSC maps (CBF, CBV and MTT). Spatial smoothing with kernel size of 4 mm full width half maximum was applied.

Paired *t*-test was performed between maps using voxel-based analysis, generating statistical parametric maps. The statistical parametric maps (*p*-values) are presented superimposed on a T1 image from a single subject to permit informative anatomical reference. We report significant voxels ($p < 0.05$). The average values in each significant cluster for each patient at each time point is extracted from the FA, MD, CBF and CBV maps, and the averages of each group were presented in a graph in each brain region. Average CBF and CBV maps of all patients were calculated, as well as delta maps comparing the two time points.

2.5. Statistical analysis

Non-parametric Wilcoxon signed ranked test was performed on the FA, MD, CBF, and CBV values in each significant cluster. Only clusters passing $p < 0.05$ in the non-parametric statistical analysis are reported.

3. Results

Of the 10 patients recruited for the study, three were lost to follow up, leaving seven patients in the final study population. The mean age of the study population was 51 years (standard deviation = 13.14), six (85.7%) of whom were male. More details regarding the study population are described in Table 1.

3.1. Regional brain microstructure integrity

FA and MD whole brain statistical maps are depicted in Figs. 1 and 2, respectively, and show both increases and decreases in FA and MD. Increases in both FA and MD are presented as orange–yellow clusters whereas decreases in FA and MD are presented as cyan clusters. Wilocoxon *p*-values are shown in Table 2. Only regions passing the threshold of $p < 0.05$ in Wilocoxon signed-rank test are presented.

A statistically significant increase in FA was found in regions related to cognition, including memory (hippocampus, medial temporal lobe) visual perception (fusiform, medial occipital gyrus) language (angular gyrus, inferior parietal lobule). A decrease in FA was found in frontal white matter and sensory-motor regions (precentral gyrus and superior corona radiata). Graphs of averages and standard errors for FA in significant clusters are presented in Fig. 3.

A decrease in MD was found in cognition related regions, including memory (hippocampus, temporal regions) and visual perception (fusiform, occipital regions). An increase in MD was found in frontal regions and in the thalamus (Fig. 2). Graphs of averages and standard errors in significant clusters are presented in Fig. 3.

3.2. Increased brain perfusion

Brain perfusion was quantified using DSC parameters (CBF and CBV). Average CBV and CBF and delta whole brain maps are depicted in Fig. 4 and show the increase in both CBF and CBV following CPAP treatment.

3.3. Regional changes in brain perfusion

Statically significant increase in CBF following CPAP treatment involved body of corpus callosum, temporal regions (inferior temporal gyrus, middle and superior temporal pole), and occipital inferior gyrus (Fig. 5(a)). No significant decrease in CBF in any brain region was found. Graphs of averages and standard errors CBF in significant clusters are presented in Fig. 6(a) presenting only regions passing the threshold of $p < 0.05$ in Wilocoxon signed-rank test.

A statistically significant increase in CBV was found in genu of corpus callosum, medial temporal gyrus, superior parietal gyrus, pallidum and putamen (Fig. 5(b)). No significant decrease in CBV in any brain region was found. Graphs of averages and standard errors CBV in significant clusters are presented in Fig. 6(b) presenting only regions passing the threshold of $p < 0.05$ in Wilocoxon signed-rank test.

3.4. Corrections for multiple comparisons

When applying correction for multiple comparisons the following regions pass the statistical threshold ($p < 0.05$, corrected) for increased FA: fusiform, hippocampus, and medial temporal lobe. Similarly, correction for multiple comparisons for increased CBV indicated that the following regions continued to pass the statistical threshold ($p < 0.05$, corrected): superior parietal gyrus, medial temporal gyrus. Decrease in FA, changes in MD, changes in CBF, and decrease in CBV did not pass correction for multiple comparisons.

4. Discussion

The present study demonstrates CPAP treatment-induced changes in brain structure and perfusion in OSA patients by comparing brain scans obtained prior to, and following CPAP

Table 1
Study population characteristics.

Characteristics	Study population ($N = 7$)
Age (years)	51 ± 13.14
Male, *n* (%)	6 (85.7)
BMI	35.23 ± 2.59
Epworth Sleepiness Scale	14.86 ± 4.74
Time between brain scans (days)	124.71 ± 30.61
A + H events during PSG, *n* (*n*/h)	355.86 ± 192.52 (57.3 ± 26.74)
Oxygen desaturation events during PSG, *n* (*n*/h)	315.14 ± 173.37 (50.13 ± 23.51)
Diabetes, *n* (%)	4 (57.1)
Heart disease, *n* (%)	4 (57.1)
Hypertension, *n* (%)	3 (42.7)
Dyslipidemias, *n* (%)	3 (42.7)
Atrial fibrillation, *n* (%)	1 (14.3)
Sarcoidosis, *n* (%)	1 (14.3)
History of pulmonary embolism, *n* (%)	1 (14.3)

A + H, apneic + hypopneic events; BMI, body mass index; PSG, polysomnography; n/h, number per hour.

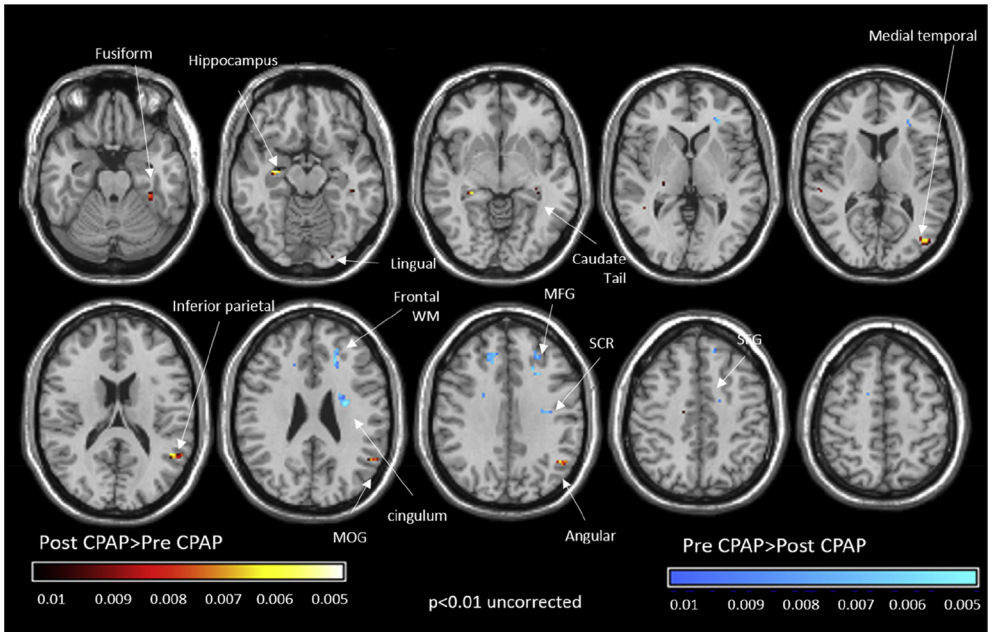

Fig. 1. Whole brain diffusion tensor imaging (DTI) functional anistrophy (FA) statistical parametric maps. Increase in FA is depicted in yellow–orange clusters and decrease in FA in cyan clusters ($p < 0.01$ uncorrected). Increase in FA was found in regions related to cognition, including memory (hippocampus, medial temporal lobe) visual perception (fusiform, medial occipital gyrus) language (angular gyrus, inferior parietal lobule). Decrease in FA was found in frontal white matter, sensory-motor regions (precentral gyrus and superior corona radiata). MFG, middle frontal gyrus; MOG, middle occipital gyrus; SCR, superior corona radiate; SFG, superior frontal gyrus, WM, white matter.

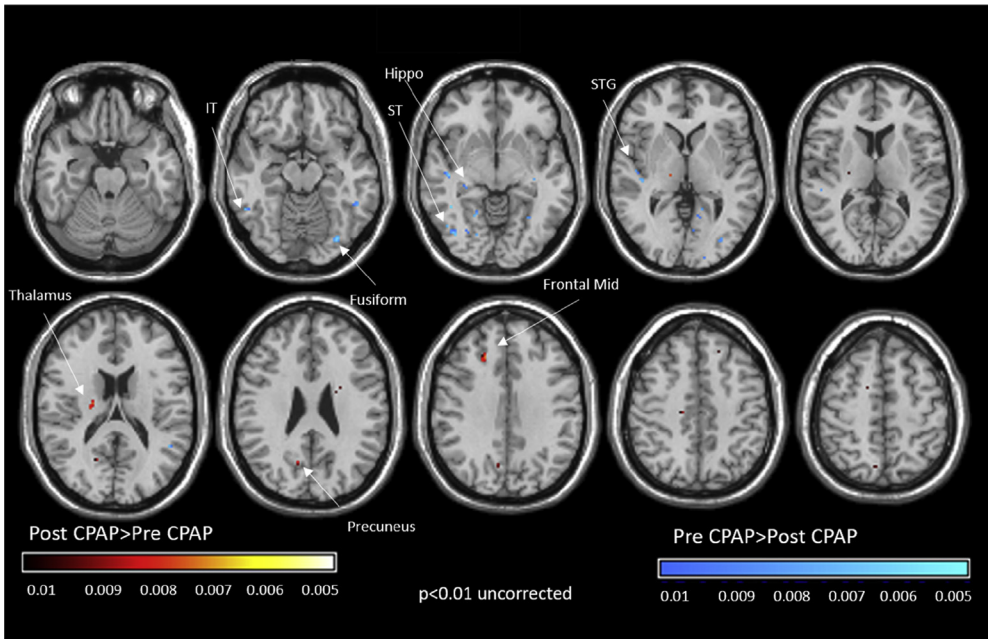

Fig. 2. Whole brain diffusion tensor imaging (DTI) mean diffusivity (MD) statistical parametric maps. Increase in MD is depicted in yellow–orange clusters and decrease in MD in cyan clusters ($p < 0.01$ uncorrected). Decrease in MD was found in cognition-related regions, including memory (hippocampus, temporal regions, visual perception regions (fusiform, occipital regions)). Increase in MD was found in frontal regions and in the thalamus. IT, inferior temporal; SFG, superior frontal gyrus; SCR, superior corona radiate; ST, superior temporal; STG, superior temporal gyrus.

treatment. Our chosen imaging modality allowed for quantification of regional brain microstructural integrity and cellularity, CBF, and CBV. Study results show several post-CPAP brain changes, namely: (1) increases and decreases in FA, representing changes in brain microstructure, (2) increases and decreases in MD, representing changes in brain cellularity, edema, and necrosis, and (3) increases in both CBF and CBV, representing increases in brain perfusion capability. Furthermore, the observed increases in FA were associated with corresponding decreases in MD, which were observed in regions of the brain relating to cognition, memory, vision, and

Table 2
List of regions presenting significant change following continuous positive airway pressure in functional anistrophy (FA), mean diffusivity (MD), cerebral blood flow (CBF) and cerebral blood volume (CBV).

Brain region	MNI coordinates			*p*-Value (Wilcoxon)	Cluster size
	x	*y*	*z*		
FA increase					
Fusiform L	−31.5	−34.5	−19.5	0.0156	155
Hippocampus R	33	−12	−15	0.0156	32
Medial temporal L	−51	−57	22.5	0.0156	151
Medial occipital L	−37.5	−72	30	0.0156	25
Angular L	−43.5	−58.5	34.5	0.0156	31
Inferior parietal L	−52.5	−28.5	37.5	0.0156	23
Lingual L	−28.5	−90	−18	0.0313	
Inferior occipital L	−18	−93	−12	0.0313	63
Caudate tail	−33	−31.5	−4.5	0.0313	26
FA decrease					
Frontal white matter	−27	−6	25.5	0.0313	57
Anterior cingulum	−18	31.5	28.5	0.0156	280
Medial frontal L	−19.5	25.5	36	0.0156	
Superior frontal R	10.5	37.5	37.5	0.0156	167
Precentral gyrus R	19.5	40.5	45	0.0156	
Superior corona radiata L	−36	−12	31.5	0.0313	45
MD increase					
Precuneus R	15	−63	21	0.0313	54
Thalamus R	16.5	−18	3	0.0156	32
Frontal Mid L	−27	30	31.5	0.0156	42
Frontal cortex BA 9	−16.5	37.5	22.5	0.0469	38
MD decrease					
Superior temporal R	51	−31.5	9	0.0156	28
Hippocampus R	30	−27	−9	0.0469	46
Internal capsule R	36	−28.5	−1.5	0.0469	
Temporal Inf L	−49.5	−46.5	−15	0.0297	25
Temporal Sup R	51	−15	−7.5	0.0297	60
Temporal Sup R	48	−13.5	1.5	0.0469	
Fusiform_L	−30	−78	−13.5	0.0313	20
CBF increase					
Body of cc	16.5	−63	49.5	0.0156	23
Inferior occipital R	51	−63	22.5	0.0469	6
Inferior Temporal R	0	13.5	18	0.0156	2
CBV increase					
Parietal Sup R	16.5	−63	49.5	0.0156	12
Temporal Mid R	51	−63	22.5	0.0313	12
Body of cc	0	13.5	18	0.0156	11
Pallidum R	18	1.5	−6	0.0469	13
Putamen L	−10.5	7.5	−9	0.0156	7

p-Values follow Wilcoxon signed rank test. BA, Brodmann area; cc, corpus callosum.
Inf, inferior; L, left; Mid, middle; MNI, Montreal Neurological Institute; R, right; Sup, superior.

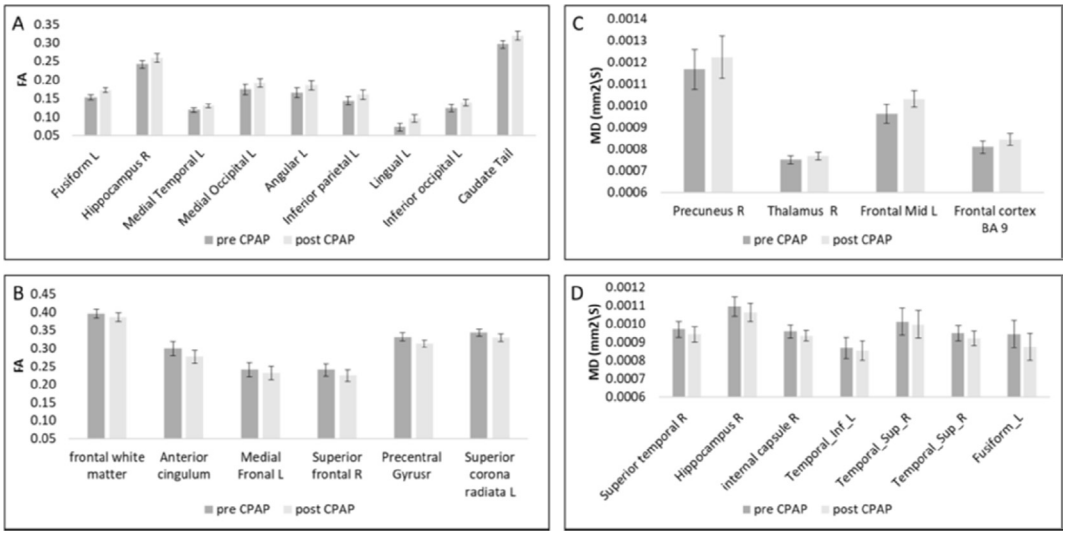

Fig. 3. Diffusion tensor imaging (DTI) averages and standard errors in significant clusters. (a) Increase in functional anistrophy (FA) following continuous positive airway pressure (CPAP). (b) Decrease in FA following CPAP. (c) Increase in mean diffusivity (MD) following CPAP. (d) Decrease in MD following CPAP. L, left; R, right.

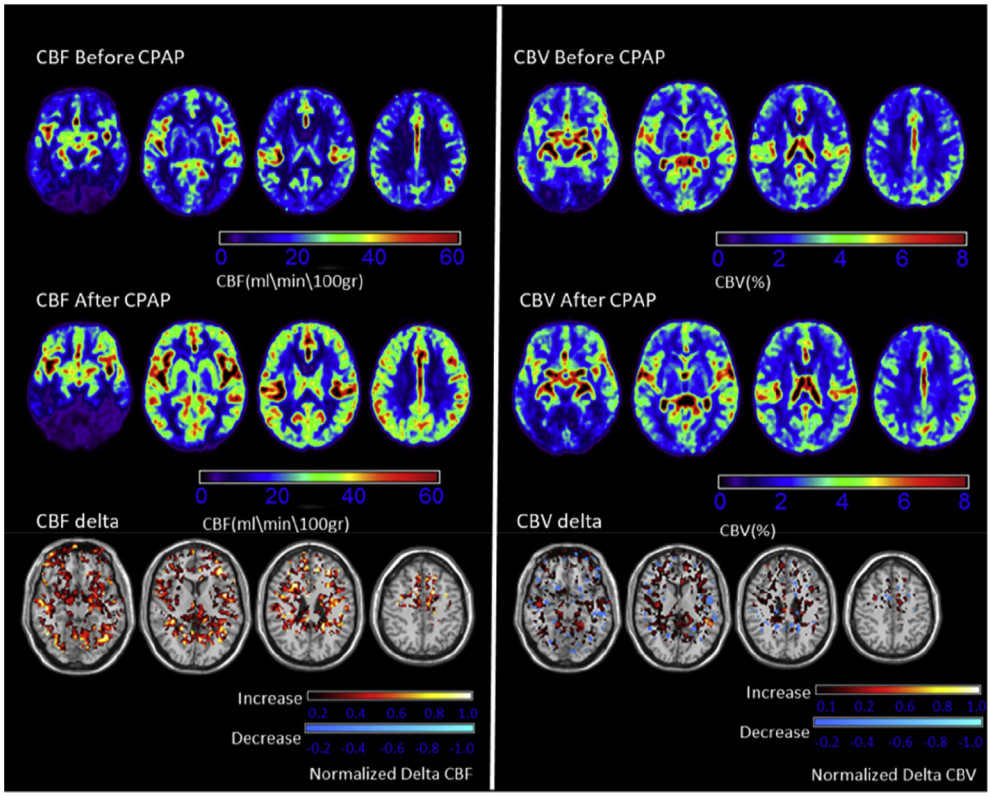

Fig. 4. Average cerebral blood volume (CBV) and cerebral blood flow (CBF) and delta whole-brain maps showing increase in CBF and CBV. CPAP, continuous positive airway pressure.

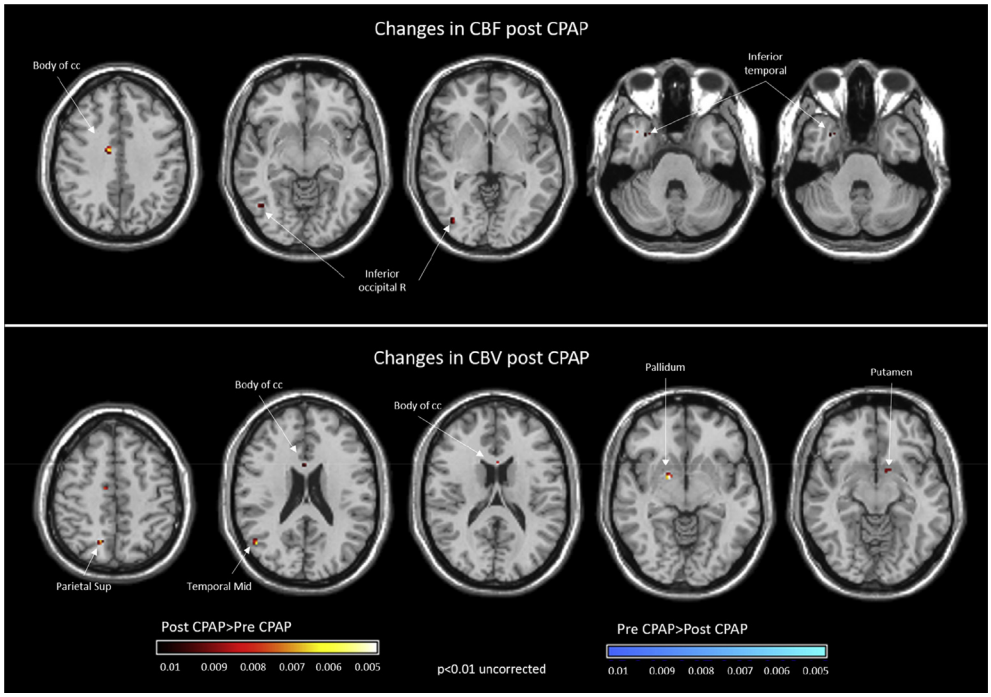

Fig. 5. Whole brain dynamic susceptibility contrast (DSC) cerebral blood flow (CBF) and cerebral volume (CBV) Statistical parametric maps. Increase in CBF and CBV is depicted in yellow–orange clusters. No significant decrease in CBF and CBV was found ($p < 0.01$ uncorrected). Increase in CBF was found in cognition-related regions, including memory (hippocampus, temporal regions, visual perception regions (fusiform, occipital regions)). Increase in CBV was found in frontal regions and in the thalamus. cc, corpus callosum; Mid, middle; CPAP, continuous positive airway pressure; R, right; Sup, superior.

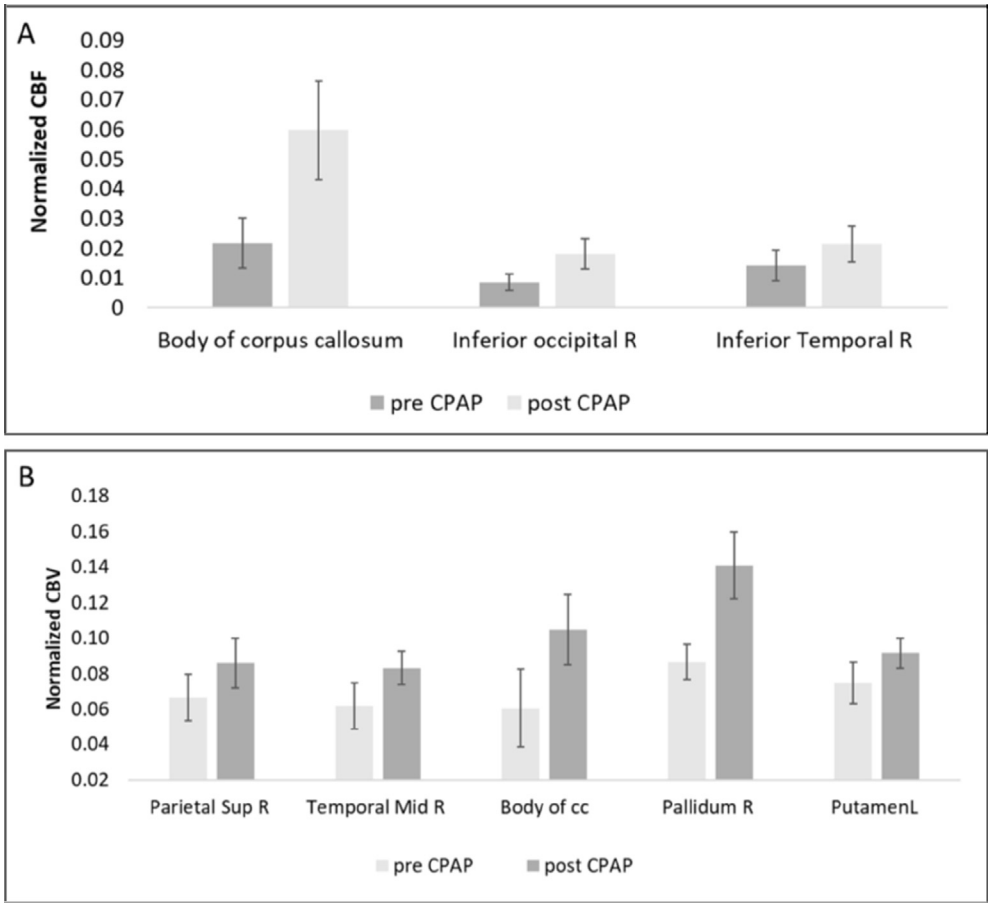

Fig. 6. Dynamic susceptibility contrast (DSC) averages and standard errors in significant clusters. (a) Increase in normalized cerebral blood flow (CBF) following continuous positive airway pressure (CPAP). (b) Decrease in normalized cerebral blood volume (CBV) following CPAP. cc, corpus callosum; L, left; Mid, middle; R, right; Sup, superior.

language. Similarly, decreases in FA were accompanied by corresponding increases in MD, as were observed in regions of the brain relating to sensory and motor functions.

Sufficient oxygen delivery to the brain, the highest oxygen-consuming organ in the body, is critical. Autoregulatory mechanisms exist in order to ensure proper oxygen delivery to the brain, namely decreased oxygen levels promote cerebral vasodilation in order to increase CBF and oxygen delivery to the brain [42]. Decreased oxygenation associated with OSA, however, results in reduced CBF, not increased CBF [11]. This occurs because the limited oxygen availability associated with OSA creates a state of persistent oxygen deprivation, leading damage of the cerebral vasculature and loss of autoregulatory mechanisms [8,11]. Continued hypoxia results in reactive oxygen species (ROS) production, which may further limit brain repair mechanisms [8]. CPAP treatment, however, addresses the source of the problem by reversing the mechanism underlying hypoxia, thus increasing oxygenation. This likely limits ROS production, a factor contributing to hypoxia-induced cellular damage, which can then allow for the activation of the brain's repair mechanisms.

This repair mechanism activation could lead to improvements in the brain's microstructural integrity, and therefore explain our observed increases in FA in the hippocampus, medial temporal lobe, fusiform gyrus, and inferior parietal lobule. Similarly, this would decrease the damage present in the brain, thus explaining the observed decreases in MD in the hippocampus, temporal regions, fusiform, and occipital regions. Unexpected findings were as follows: (1) decreased FA in the frontal white matter and sensory-motor regions and (2) increased MD in the frontal regions and the thalamus. Past literature has indicated that white matter structures heal at a slower rate than other neural structures, with even 1 year not being a sufficient time interval to observe desired improvements [37]. Furthermore, higher blood flow and volume may alter water diffusivity in the brain tissue [43] in which case the decreases in FA and increases in MD may be due to the observed increases in CBF and CBV.

The increases in CBF and CBV suggest improvements in cerebral vasculature. Studies have shown that CPAP treatment increased muscular sympathetic nerve activity [24] and cerebrovascular reactivity [22], which indicates restoration of the vasodilatory mechanisms lost in patients with OSA and also explains the post-CPAP observed increases in CBF and CBV. Angiogenesis has been suggested to play a role in other forms of brain injury repair [34]. Although its application to OSA-induced brain injury has not yet been studied, this may further explain the increased CBF and CBV. Finally, locations of DTI, CBF, and CBV changes do have a lot of overlap, particularly in regard to cerebral changes. However, there are some differences, such as increased CBF and CBV the corpus callosum, but lack of corresponding DTI changes. This may be due to CBF and CBV's overall effect on increasing water diffusivity, which can have downstream effects throughout the brain. Alternatively, it is possible that there are actually more changes beyond those detected, but that were not statistically significant due to our small sample size.

Past research has focused mainly on using T1 and T2 weighted MRI to evaluate structural brain changes [23–25,27]. For instance,

by comparing OSA patients receiving CPAP to those not receiving CPAP, Rosenzweig et al., observed baseline hypotrophic changes in the hippocampus, bilateral pallidus, right thalamus, and mid-posterior part of the corpus callosum on neuroimaging in patients with OSA compared to the controls [23]. Thus, they suggested that CPAP treatment reduced these hypotrophic changes until there was no significant difference between OSA patients and controls [23]. Our methodology differed from Rosenzweig et al., in that we utilized a pre- and post-treatment design in contrast to their treatment and control, but we observed all the same changes that Rosenzweig et al., observed, thus confirming our results. However, we observed additional changes in the temporal lobes, fusiform gyrus, occipital regions, angular gyrus, parietal lobes, frontal regions, and corona radiata that were not observed by Rosenzweig et al., these differences are likely due to our imaging modality being more sensitive and advanced than traditional T1 and T2 weighted MRI, thus allowing for more detailed visualization and quantification of treatment-induced changes.

More recently, a limited number of studies have been performed using DTI to assess brain structural integrity, as we did. Chen et al., used DTI to compare brain microstructure in patients with OSA compared to controls, for which they observed significantly reduced global brain FA levels as well as an association between white matter damage and disease severity [36]. However, they did not include post-CPAP treatment scans and analyses in their study. Conversely, Xiong et al., used DTI to assess post-treatment structural changes, although their primary comparison was between patients with and without residual sleepiness following CPAP treatment [35]. Neither of these studies, however, include and pre- and post-treatment design, as does our study. Only Castronovo et al., [37] utilized a pre- and post-treatment design similar to our own, although they also correlated brain structure changes to cognitive performance, which we did not do. Yet, whereas Castronovo et al., observed changes in FA and MD in the parietal and frontal regions, but not elsewhere in the brain, we observed the same changes in the frontal regions, but not the parietal regions. Alternately, we observed additional changes throughout the brain beyond that detected by Castronovo et al., [37].

Furthermore, while other studies have assessed CPAP-induced perfusional changes, none of these previous studies have utilized DSC imaging to do so, as we did. Jimenez-Caballero et al., measured brain perfusion using cervical and transcranial Doppler ultrasonography both prior to and after two years of CPAP treatment, and observed reduced cerebral blood flow velocity in OSA patients following the CPAP treatment [26]. However, they were not able to identify brain regions impacted by the CPAP-treatment as we did, due to limitations of their chosen imaging modality. Furthermore, Jimenez-Caballero et al., used an apnea test, an index of the capabilities of cerebral vessels to adapt to metabolic demands, to demonstrate an improvement in hypercapnic cerebrovascular reactivity (CVR) [26]. This explains the reason behind our observed increases in CBF and CBV following CPAP treatment. Our imaging modality, in contrast, allows for direct assessment of CBF, as opposed to cerebral blood flow velocity. Furthermore, whereas CVR is a measure of function, thereby allowing for assessment functional changes, our imaging modality allows for the assessment of structural integrity changes. Nonetheless, these studies are in agreement with one another in their assessment of CBF and CBV improvements following CPAP treatment.

Prilipko et al., [22] decided to further these results and performed a similar study to ours, but utilized fMRI to measure CVR and CBF. Our results are in agreement with the results of this study that demonstrated changes in the 'Default Mode Network,' a group of brain regions including the medial prefrontal cortex, posterior cingulate cortex, precuneus, inferior parietal lobes, medial temporal regions, hippocampus, and angular gyrus. Prilipko et al.'s use of fMRI allowed for them to draw conclusions regarding changes in brain activity whereas our use of DTI and DSC shed light on the mechanisms through which these changes occur, namely brain healing and repair. However, while Prilipko et al., observed no difference in relative CBF between OSA patients and controls, we observed post-treatment improvements in CBF. Furthermore, to the best of our knowledge, there are no other studies utilizing these parameters as opposed to standard MRI settings, making this the first study to assess CPAP treatment's effect using DTI and DSC, and therefore the first study of CPAP-induced pathophysiological changes.

Limitations include small sample size. Moreover, because of the small sample size, many of the observations became insignificant when corrected for multiple comparisons. Had the sample size been larger, this likely would not have been the case. Additionally, loss to follow up could have potentially induced selection bias into the study if the population lost differed from those remaining in the study. The study also lacked a control group. While this is generally important for demonstrating that a treatment has an effect or a stronger effect than another treatment; by comparing each patient's baseline and post-treatment scans, we consider the baseline scan equivalent to a control group and the post-treatment scan as the treatment effect. This resembles the way treatment effects are measured in cross-over studies. Furthermore, many of the patients included in the study had co-morbidities, which could have potentially confounded the results. However, if these co-morbidities had any confounding effect, we suspect that the effect would be limiting to the treatment effect, not an enhancement of the treatment effect. Therefore, the improvement in brain structure and perfusion despite these co-morbidities demonstrates the strength of CPAP treatment, and we expect that an even larger, stronger treatment effect would be seen in patients who do not have potentially limiting co-morbidities. Finally, this study is based purely on MRI scan analysis. Clinical data was not collected from the patients and therefore not compared to the radiological changes observed in the study. The small sample size and high patient drop-out rate would have made this very difficult, although this data should be gathered in future studies in order to strengthen and deepen the findings of this current study.

5. Conclusion

In addition to symptom resolution, CPAP treatment has multiple effects on brain structure and perfusion, as evidenced through DTI and DSC MRI and quantified based on the FA, MD, CBF, and CBV parameters. The increases in FA and corresponding decreases in MD occurring in the brain regions related to cognition, vision, and language indicate high myelination, dense axonal packing, and white matter maturation, which is suggestive of improved brain structure, possibly due to repair mechanisms in the brain. Similarly, the decreases in FA and corresponding increases in MD occurring due to CPAP treatment indicate decreased axonal degeneration and decreased demyelination, which is suggestive of cessation of damage occurrence. Finally, whereas reduced CBF is a hallmark of OSA, improvement in CBF and CBV suggest recovery of autoregulatory mechanisms, thereby allowing for proper vascular reactivity and vasodilation. Overall, CPAP treatment improves brain microstructural integrity and perfusion, suggestive of repair and healing of OSA-induced brain damage. Nonetheless, future research should be performed on larger study populations and in patients lacking co-morbidities to strengthen the results of this study. Further research should include clinical data to correlate to radiological changes observed as a result of treatment.

Funding disclosure

This research did not receive any specific grant from funding agencies in the public, commercial, or not-for-profit sectors. Funding for the post-processing and statistical analysis was provided by the hospital's research fund. The funding source had no involvement in any matters regarding production and publication of this manuscript.

Conflict of interest

H.S. Maresky is the CEO of a 3-D imaging research laboratory in Toronto, Ontario, Canada (Visionairy ™) and is the recipient of a grant from NVIDIA Corporation ®; however, Dr. Maresky declares no conflict of interests. H.S. Maresky, M.M. Klar, M.L., and S. Tal have a patent pending in regard to another, unrelated research project, and declare no conflicts of interest in this regard. The authors report no other disclosures or conflicts of interest. This research did not receive any specific grant from funding agencies in the public, commercial, or not-for-profit sectors. Funding for the post-processing and statistical analysis was provided by the hospital's research fund. The funding source had no involvement in any matters regarding production and publication of this manuscript.

The ICMJE Uniform Disclosure Form for Potential Conflicts of Interest associated with this article can be viewed by clicking on the following link: https://doi.org/10.1016/j.sleep.2018.12.027.

Appendix A. Supplementary data

Supplementary data to this article can be found online at https://doi.org/10.1016/j.sleep.2018.12.027.

References

[1] Young T, Palta M, Dempsey J, et al. Burden of sleep apnea: rationale, design, and major findings of the Wisconsin Sleep Cohort Study. Wis Med J 2009;108:246–9.
[2] Yaggi H, Concato J, Kernan W, et al. Obstructive sleep apnea as a risk factor for stroke and death. N Engl J Med 2005;353:2034–41.
[3] Young T, Palta M, Dempsey J, et al. The occurrence of sleep disordered breathing among middle-aged adults. N Engl J Med 1993;328:1230–5.
[4] Peppard PE, Young T, Barnet JH, et al. Increased prevalence of sleep-disordered breathing in adults. Am J Epidemiol 2013;177(9):1006–14.
[5] Tufik S, Santos-Silva R, Taddei JA, et al. Obstructive sleep apnea syndrome in the Sao Paulo Epidemiologic sleep study. Sleep Med 2010;11(5):441–6.
[6] Young T, Finn L, Peppard P, et al. Sleep disordered breathing and mortality: Eighteen-year follow-up of the Wisconsin sleep cohort. Sleep 2008;31(8):1071–8.
[7] Golbin JM, Somers VK, Caples SM. Obstructive sleep apnea, cardiovascular disease, and pulmonary hypertension. Proc Am Thorac Soc 2008;5(2):200–6.
[8] Urbano F, Roux F, Schindler J, et al. Impaired cerebral autoregulation in obstructive sleep apnea. J Appl Physiol 2008;105(6):1852–7.
[9] Neelapu BC, Kharbanda OP, Sardana HK, et al. Craniofacial and upper airway morphology in adult obstructive sleep apnea patients: a systematic review and meta-analysis of cephalometric studies. Sleep Med Rev 2017;31:79–90.
[10] Chi L, Comyn FL, Mitra N, et al. Identification of craniofacial risk factors for obstructive sleep apnea using three- dimensional MRI. Eur Respir J 2011;38(2):348–58.
[11] Yadav SK, Kumar R, Macey PM, et al. Regional cerebral blood flow alterations in obstructive sleep apnea. Neurosci Lett 2013;555:159–64.
[12] Young T, Peppard P, Gottlieb D. Epidemiology of obstructive sleep apnea: a population health perspective. Am J Respir Crit Care Med 2002;165:1217–39.
[13] Feliciano M, Torres V, Vaz F, et al. Overview of proteomic studies in obstructive sleep apnea. Sleep Med 2015;16(4):437–45.
[14] Pepperell J, Ramdassingh-Dow S, Crosthwaite N, et al. Ambulatory blood pressure after therapeutic and subtherapeutic nasal continuous positive airway pressure for obstructive sleep apnoea: a randomised parallel trial. Lancet 2002;359:204–10.
[15] Becker H, Jerrentrup A, Ploch T, et al. Effect of nasal continuous positive airway pressure treatment on blood pressure in patients with obstructive sleep apnea. Circulation 2003;107:68–73.
[16] Guilleminault C, Connolly S, Winkle R. Cardiac arrhythmia and conduction disturbances during sleep in 400 patients with sleep apnea syndrome. Am J Cardiol 1983;52:490–4.
[17] Grimm W, Koehler U, Fus E, et al. Outcome of patients with sleep apnea-associated severe bradyarrhythmias after continuous positive airway pressure therapy. Am J Cardiol 2000;86:688–92.
[18] Becker H, Brandenburg U, Peter J, et al. Reversal of sinus arrest and atrioventricular conduction block in patients with sleep apnea during nasal continuous positive airway pressure. Am J Respir Crit Care Med 1995;151:215–8.
[19] Kaneko Y, Floras J, Usui K, et al. Cardiovascular effects of continuous positive airway pressure in patients with heart failure and obstructive sleep apnea. N Engl J Med 2003;348:1233–41.
[20] Mansfield D, Gollogly N, Kaye D, et al. Controlled trial of continuous positive airway pressure in obstructive sleep apnea and heart failure. Am J Respir Crit Care Med 2004;169:361–6.
[21] Kushida CA, Nichols DA, Holmes TH, et al. Effects of continuous positive airway pressure on neurocognitive function in obstructive sleep apnea patients: the Apnea Positive Pressure Long-term Efficacy Study (APPLES). Sleep 2012;35(12):1593–602.
[22] Prilipko O, Huynh N, Thomason ME, et al. An fMRI study of cerebrovascular reactivity and perfusion in obstructive sleep apnea patients before and after CPAP treatment. Sleep Med 2014;15(8):892–8.
[23] Rosenzweig I, Glasser M, Crum WR, et al. Changes in neurocognitive architecture in patients with obstructive sleep apnea treated with continuous positive airway pressure. EBioMedicine 2016;7:221–9.
[24] Henderson LA, Fatouleh RH, Lundblad LC, et al. Effects of 12 months continuous positive airway pressure on sympathetic activity related brainstem function and structure in obstructive sleep apnea. Front Neurosci 2016;10:1–11.
[25] Xu H, Wang H, Guan J, et al. Effects of continuous positive airway pressure on neurocognitive architecture and function in patients with obstructive sleep apnoea: study protocol for a multicentre randomised controlled trial. BMJ Open 2017;7:e014932.
[26] Jiménez Caballero PE, Coloma Navarro R, Ayo Martín O, et al. Cerebral hemodynamic changes in obstructive sleep apnea syndrome after continuous positive airway pressure treatment. Sleep Breath 2013;17(3):1103–8.
[27] Dalmases M, Solé-Padullés C, Torres M, et al. Effect of CPAP on cognition, brain function, and structure among elderly patients with OSA a randomized pilot study. Chest 2015;148(5):1214–23.
[28] Artzi M, Liberman G, Nadav G, et al. Human cerebral blood volume measurements using dynamic contrast enhancement in comparison to dynamic susceptibility contrast MRI. Neuroradiology 2015;57(7):671–8.
[29] Dijkhuizen RM, van der Marel K, Otte WM, et al. Functional MRI and diffusion tensor imaging of brain reorganization after experimental stroke. Transl Stroke Res 2012;3(1):36–43.
[30] Edlow BL, Wu O. Advanced neuroimaging in traumatic brain injury. Semin Neurol 2012;32(4):374–400.
[31] Alexander AL, Lee JE, Lazar M, et al. Diffusion tensor imaging of the brain. Neurotherapeutics 2007;4(3):316–29.
[32] Brody DL, Mac Donald CL, Shimony JS. Current and future diagnostic tools for traumatic brain injury. CT, conventional MRI, and diffusion tensor imaging. 1st ed., vol. 127. Elsevier B.V.; 2015.
[33] Tal S, Hadanny A, Berkovitz N, et al. Hyperbaric oxygen may induce angiogenesis in patients suffering from prolonged post-concussion syndrome due to traumatic brain injury. Restor Neurol Neurosci 2015;33(6):943–51.
[34] Tal S, Hadanny A, Sasson E, et al. Hyperbaric oxygen therapy can induce angiogenesis and regeneration of nerve fibers in traumatic brain injury patients. Front Hum Neurosci 2017;11:1–12.
[35] Xiong Y, Zhou XJ, Nisi RA, et al. Brain white matter changes in CPAP-treated obstructive sleep apnea patients with residual sleepiness. J Magn Reson Imag 2017;45(5):1371–8.
[36] Chen H-L, Lu C-H, Lin H-C, et al. White matter damage and systemic inflammation in obstructive sleep apnea. Sleep 2015;38(3):361–70.
[37] Castronovo V, Scifo P, Castellano A, et al. White matter integrity in obstructive sleep apnea before and after treatment. Sleep 2014;37(9):1465–75.
[38] Klingelhofer J, Hajak G, Sander D, et al. Assessment of intracranial hemodynamics in sleep-apnea syndrome. Stroke 1992;23(10):1427–33.
[39] Leemans A, Jeurissen B, Sijbers J, et al. Explore DTI: a graphical toolbox for processing, analyzing, and visualizing diffusion MR data. In: 17th annual meeting of Intl Soc Mag Reson Med. Hawaii, USA; 2009. p. 3537.
[40] Ostergaard L, Weisskoff R, Chesler D, et al. High resolution measurement of cerebral blood flow using intravascular tracer bolus passages. Part I: mathematical approach and statistical analysis. Magn Reson Med 1996;36:715–25.
[41] Ostergaard L, Sorensen A, Kwong K, et al. High resolution measurement of cerebral blood flow using intravascular tracer bolus passages. Part II: experimental comparison and preliminary results. Magn Reson Med 1996;36:726–36.
[42] Cipolla MJ. Control of cerebral blood flow. In: The cerebral circulation. San Rafael, CA: Mogan & Claypool Life Scienes; 2009. https://www.ncbi.nlm.nih.gov/books/NBK53082/.
[43] Le Bihan D, Breton E, Lallemand D, et al. Separation of diffusion and perfusion in intravoxel incoherent motion MR imaging. Radiology 1988;168(2):497–505.